THE JOURNAL OF BIOLOGICAL CHEMISTRY VOL. 285, NO. 53, pp. 42013–42022, December 31, 2010

Transcription Factor Redundancy Ensures Induction of the Antiviral State*[S]

Received for publication, July 19, 2010, and in revised form, October 11, 2010 Published, JBC Papers in Press, October 13, 2010, DOI 10.1074/jbc.M110.165936

Sonja Schmid[‡], Markus Mordstein[§], Georg Kochs[§], Adolfo García-Sastre[‡¶‖], and Benjamin R. tenOever[‡¶1]

From the [‡]Department of Microbiology, the [¶]Global Health and Emerging Pathogens Institute, and the [‖]Department of Medicine, Division of Infectious Diseases, Mount Sinai School of Medicine, New York, New York 10029 and the [§]Department of Virology, University of Freiburg, Hermann-Herder-Strasse 11, D-79104 Freiburg, Germany

The transcriptional response to virus infection is thought to be predominantly induced by interferon (IFN) signaling. Here we demonstrate that, in the absence of IFN signaling, an IFN-like transcriptome is still maintained. This transcriptional activity is mediated from IFN-stimulated response elements (ISREs) that bind to both the IFN-stimulated gene factor 3 (ISGF3) as well as to IFN response factor 7 (IRF7). Through a combination of both *in vitro* biochemistry and *in vivo* transcriptional profiling, we have dissected what constitutes IRF-specific, ISGF3-specific, or universal ISREs. Taken together, the data presented here suggest that IRF7 can induce an IFN-like transcriptome in the absence of type-I or -III signaling and therefore provides a level of redundancy to cells to ensure the induction of the antiviral state.

The type I interferon (IFN-I)[2] family is a subset of cytokines encoded by a single IFNβ gene and a tandem cluster of IFNα genes (1). The transcriptional induction of IFN-I is limited to virus-infected cells and leads to the expression of a multitude of genes, conferring antiviral and immunostimulatory functions (2, 3). Binding of IFNα and/or IFNβ to the type I IFN receptor (IFNAR) leads to phosphorylation of the signal transducer and activator of transcription 1 (STAT1) and STAT2 (4), which assemble together with interferon regulatory factor 9 (IRF9) into a multisubunit complex commonly referred to as IFN-stimulated gene factor 3 (ISGF3) (5). Aside from IFN-I, ISGF3 is activated by type III IFN (IFN-III), IFNλ1–3, an activity mediated by a different cellular receptor (6, 7). ISGF3 translocates to the nucleus and binds to the enhancers of more than 100 IFN-I-stimulated genes (ISGs), whose timely expression confers a cellular environment non-conducive to viral replication. The motif responsible for ISGF3 binding is composed of the sequence: GAAANNGAAACT, and is referred to as an IFN-stimulated response element (ISRE) (5, 8–12). As no crystal structure of ISGF3 has been solved, the exact DNA binding contacts or even the stoichiometry of the ISGF3 complex remains unclear. Based on the structures of STAT1 and IRF dimers, models for ISGF3 have been proposed in which the major and minor grooves of the ISRE are occupied by the DNA binding domains of IRF9 and STAT1 on respective sides of the DNA (13). In this model, STAT1 interacts with the hydrogen:donor:acceptor:acceptor (HDAA) groups and three repetitive methyl:acceptor:donor:acceptor (MADA) groups provided in the major groove of CTTT base pairing, in addition to the neighboring acceptor:hydrogen:acceptor (ADA) groups associated with the minor groove of A:T or T:A base pairing. The opposing minor groove of CTTT (providing AHA, ADA, ADA, and ADA contacts respectively) is occupied by IRF9 as well as the major groove of the A and T downstream base pairing (14–16). In contrast, binding of homo- and heterodimeric complexes of STAT1 and/or STAT2 is limited to inverted repeats in which HDAA contacts are required in consecutive major grooves, encoded by motifs termed IFNγ-activated sequences (GAS) (17, 18).

The sequence of the ISGF3 binding site partially overlaps with the IRF binding element (IRF-E): AANNGAAANNGAAA (14, 19). This sequence is recognized by the IRF family of transcription factors, comprising IRF1 to IRF9 and virus-encoded analogues of cellular IRFs (20). The crystal structure of different IRFs bound to a DNA target sequence demonstrated that a dimeric IRF binds to two overlapping stretches of AANNGAAA, with the two IRF molecules occupying opposite sites of the DNA double helix, making minor groove contacts (AHA) with the first two A bases, and major groove contacts (AADH, ADAM, ADAM, ADAM) with the GAAA sequence (14, 15, 21, 22). However, each family member performs its specific role in biological processes through distinct expression patterns and slightly different DNA binding specificities within the broad IRF consensus sequence (21, 23–29). While IRF9 is an integral component of ISGF3 and is essential in mediating IFN-induced transcriptional activity, two additional members, namely IRF3 and IRF7, function independently and are responsible for the induction of IFN (30, 31). Upon cellular infection, IRF3 and IRF7 are phosphorylated by nuclear factor κB kinase (IKK)-related kinase IKKϵ (also called IKK-i) or TANK-binding kinase 1 (TBK1) (32), form

* This work was supported, in whole or in part, by National Institutes of Health NIAID Grants R01AI080624 (to B. R. t. O.) and R01AI046954, U19AI083025, and U01AI082970 and by CRIP (Center for Research in Influenza Pathogenesis, HHSN266200700010C), a NIAID-funded Center of Excellence for Influenza Research and Surveillance (CEIRS) (to A. G.-S.).

[S] The on-line version of this article (available at http://www.jbc.org) contains supplemental Figs. S1–S6 and Table S1.

[1] To whom correspondence should be addressed: Mount Sinai School of Medicine, One Gustave L. Levy Place, Dept. of Microbiology, Box 1124, New York, NY 10029. Tel.: 212-241-7849; Fax: 212-534-1684; E-mail: Benjamin.tenOever@mssm.edu.

[2] The abbreviations used are: IFN-I, type I interferon; ISRE, IFN-stimulated response elements; IRF, interferon regulatory factor; ISGF, interferon-stimulated gene factor; ISG, IFN-I-stimulated gene; IRF-E, IRF binding element; hpt, hour post-transfection; PAMP, pathogen-associated molecular patterns; hpi, hour postinfection.

hetero- and homodimers, translocate to the nucleus, and transcribe IFNβ and the various IFNα genes (33). Whereas IRF3 is ubiquitously expressed (34), basal IRF7 expression is limited to hematopoietic cells, with the highest expression level in plasmacytoid dendritic cells (pDCs) (35). Other cell types upregulate IRF7 upon stimulation with IFN-I/-III and/or tumor necrosis factor α (TNFα) (36, 37). Regardless of cell type, phosphorylation and activation of IRF3 and IRF7 results in nuclear localization and binding to IRF-E sites, with IRF7 showing significantly more promiscuity with regards to IRF-E variation (30). The IRF3-specific transcriptome that results following IRF3 activation has been determined and compromises a small subset of genes, most notably IFNβ (38–41). In addition, similar studies focusing on the transcriptional potential of IRF7 have also been performed and yielded similar results, albeit demonstrating a greater diversity of genes mediated by both autocrine IFN-I signaling and the greater binding capacity of IRF7 (42). Taken together, it is widely accepted that IRF3 and IRF7 are essential components required for the establishment of the antiviral state, with their primary function residing in the activation of ISGF3 through the synthesis of IFN-I and/or IFN-III.

In an effort to determine the *in vivo* contribution of IFN-I/-III to the antiviral response, we performed influenza A virus infections in mice encoding genetic disruptions in the receptors for both IFN-I and -III signaling (43). Surprisingly, transcriptional profiling of infected lung tissue revealed that a significant portion of virus-induced genes were "interferon-stimulated genes" despite the complete absence of ISGF3 activation. Given this intriguing discovery, we sought to determine the functional redundancy between the transcriptomes of ISGF3 and IRFs, most notably IRF7. To address this question, we systematically compared binding of IRF7 and ISGF3 to a variety of ISRE motifs encoded upstream of the transcriptional start sites of those "ISGs" induced in the absence of IFN signaling. Here we demonstrate that IRF7 and ISGF3 can engage identical DNA motifs and also define the properties that confer IRF7 and/or ISGF3 specificity. Furthermore, we define the IRF7 transcriptome in the absence of IFN-I and IFN-III signaling. Taken together, we find a significant overlap between the genes induced by IRF7 and ISGF3 suggesting that transcription factor redundancy evolved to ensure the induction of the antiviral state.

EXPERIMENTAL PROCEDURES

Virus—We used the recombinant influenza A virus strains SC35M wild type (SC35M-wt), SC35M-ΔNS1 (44), deficient in the nonstructural protein 1 (NS1), and PR/8/34 NS1-R38AK41A (45), harboring two amino acid substitutions in NS1.

Mice and Viral Infections—B6.A2G-*Mx1-IFNAR1*$^{-/-}$-*IL28Rα*$^{-/-}$ mice (43), carrying intact Mx1 alleles and defective alleles for *IFNAR1* and *IL28Rα* were bred locally, in accordance with institution animal care guidelines. Mice were anesthetized by intraperitoneal injection of a mixture of ketamine (100 μg per gram body weight) and xylazine (5 μg per gram body weight) before intranasal infection with 10^5 plaque forming units (pfu) of either SC35M-wt or SC35M-ΔNS1 in 50 μl of PBS containing 0.3% BSA. Animals treated with PBS/0.3% BSA served as negative controls.

Cell Culture and Reagents—HEK293T, 2FTGH, U3A (46), and A549 cells were cultured in Dulbecco's modified Eagle's medium (DMEM, Invitrogen) supplemented with 10% fetal bovine serum (FBS) and 1% penicillin/streptomycin. Primary murine embryonic fibroblasts (MEFs) were derived from pools of Irf3$^{-/-}$, Irf7$^{-/-}$, or Irf3$^{-/-}$Irf7$^{-/-}$ knock-out mice and were a kind gift of Michael S. Diamond (Washington University School of Medicine). Primary MEFs were also cultured in DMEM supplemented with 10% FBS and 1% penicillin/streptomycin. Transfection of DNA was performed with Lipofectamine 2000 (Invitrogen). siRNA against human IRF3 (Santa Cruz Biotechnology) was transfected at a final concentration of 50 nM in Opti-MEM I-reduced serum medium (Invitrogen), using Lipofectamine RNAiMAX (Invitrogen) according to the manufacturers' instructions. Where indicated, cells were treated with 15–30 IU/ml of human IFNβ (BEI resources). For inhibition of translation, primary MEFs were treated with 100 μg/ml of cycloheximide (Sigma). 1×10^6 primary MEFs or 3×10^6 A549 cells were transfected with 4 μg or 24 μg respectively of poly(I:C) (Sigma) using Lipofectamine 2000. Infection of cells with PR/8/34 NS1-R38AK41A, was performed at a multiplicity of infection (MOI) of 5 in complete medium.

Plasmids—Mammalian expression plasmids encoding flag-tagged human IRF3, IRF7, IRF9, STAT1, and STAT2 were generated using the multiple cloning site (MCS) of the pCAGGS plasmid (47). An expression plasmid for Flag-tagged human IKKε was generated by inserting the open reading frame (ORF) of IKKε into MCS of pFlag-CMV2 (Sigma). The reporter construct encoding for firefly luciferase under control of the human ISG15-ISRE was constructed, by inserting an annealed oligonucleotide harboring the ISG15-ISRE sequence (forward: 5′-AGCTTCTCGGGAAAGGGAAACCGAAACTGAAGC-3′; reverse: 5′-TCGAGCTTCAGTTTCGGTTTCCCTTTCCCGAGA-3′) into the MCS of pLuc-MCS (Stratagene). To generate cells stably expressing GFP, IRF7, or STAT1 a lentiviral vector was used. The respective ORFs were inserted into a minimal HIV-1 provirus termed V1 (48) via the restriction enzyme SfiI.

Luciferase Assay—2×10^5 HEK293T cells were transfected with 0.1 μg per expression plasmid together with 0.2 μg of the ISG15-ISRE-dependent luciferase construct and 10 ng of a construct constitutively expressing *Renilla* luciferase to normalize for transfection efficiency. Empty vector served to fill up each transfection reaction to 0.6 μg of total plasmid. 14 h post-transfection (hpt) medium was changed and 15 IU/ml of IFNβ was added. Luciferase activity was determined 24 hpt using the dual-luciferase reporter assay system (Promega).

Electrophoretic Mobility Shift Assay (EMSA)—2×10^6 HEK293T cells were transfected with 1 μg per expression plasmid and empty vector served to fill up each transfection reaction to 4 μg of total plasmid. 14hpt medium was changed and 15 IU/ml of IFNβ was added. Whole cell extracts were obtained 24 hpt, and EMSAs were performed as described previously (13). For supershift analysis, 1 μg of antibody, specific to STAT1α p91 (C-111), STAT2 (H-190), ISGF3γ p48

(H-143), IRF3 (FL-425), IRF7 (G-8) (all purchased from Santa Cruz Biotechnology), Flag (M2, Sigma), or control IgG was used.

Western Blot Analysis—Western blot analysis was performed as previously described (49). Antibodies specific to β-actin (Abcam), Flag (M2), STAT1α p91 (C-111), IRF3 (FL-425), and IRF7 (G-8, Santa Cruz Biotechnology) were all used at a concentration of 1 μg/ml and antibodies specific to ISG56 (Thermo Scientific) and MxA were used at a 1:1000 dilution.

Quantitative PCR (qPCR)—qPCR was performed as previously described (49). Primers used for qPCR can be found in supplemental Table S1.

Affymetrix Analysis—Both affymetrix analyses were performed at the biopolymers facility at Harvard Medical School, and data were analyzed on the gene pattern server. Lungs from infected and mock-treated mice were harvested at the indicated time points and total RNA was isolated. RNA from three lungs per cohort was pooled to perform standard affymetrix analysis. The heat map depicts a subset of genes that were induced in Flu-ΔNS1-infected samples at least three times over mock-treated samples. The complete data of the affymetrix analysis can be found at NCBI GEO, with the accession number GSE24695. For analysis of IRF7-driven genes in U3A cells, U3A cells were transfected with expression plasmids encoding for Flag-tagged IRF7 and Flag-tagged IKKϵ in a ratio of 1:1. Control U3A cells were transfected with a GFP-encoding plasmid. 4 hpt, medium was changed and 25 IU/ml of type I IFN was added. Total RNA was isolated 20 hpt. Standard affymetrix analysis was performed in replicates on U133A 2.0 affymetrix chips. Genes, significantly ($p < 0.05$) up-regulated at least 2-fold in samples transfected with IRF7 and IKKϵ are shown in the heat map. ISGs were identified with the INTERFEROME database.

RESULTS

Profiling Virus-induced Genes in the Absence of IFN-I and -III Signaling—Cells detect invading viruses by recognizing pathogen-associated molecular patterns (PAMPs) with specific receptors, leading to activation of several signaling pathways ultimately resulting in the induction of IFN-I and -III. Autocrine and paracrine signaling of IFNs in response to PAMP detection results in the up-regulation of ~100 antiviral genes, generating a cellular environment non-conducive to productive virus infection. To identify virus-inducible, IFN-independent genes, we treated knock-out mice, deficient for both functional type I and III IFN receptors (IFNAR1$^{-/-}$IL28Rα$^{-/-}$) with recombinant influenza A virus strains, which were either wild type (Flu-wt) or lacked the IFN-antagonistic viral product NS1 (Flu-ΔNS1) (43, 50, 51). 12, 24, and 48 h postinfection (hpi), lungs of infected and uninfected mice were harvested, and total RNA was isolated. As expected, lungs from Flu-ΔNS1-infected mice demonstrated strong transcriptional induction of IFNβ and IFNλ2 mRNA after 24 and 48 hpi as compared with Flu-wt infections (Fig. 1*A*). Transcriptional induction of IFN was not the result of differences in viral load as levels of nucleoprotein (NP) mRNA were comparable at each time point analyzed between both viral cohorts (Fig. 1*A*). RNA derived from pooled lungs of ΔNS1 infected mice were extracted and analyzed by affymetrix-based microarray. Fig. 1*B* depicts a subset of genes up-regulated at least 3-fold in IFNAR1$^{-/-}$IL28Rα$^{-/-}$ mice infected, as compared with un-

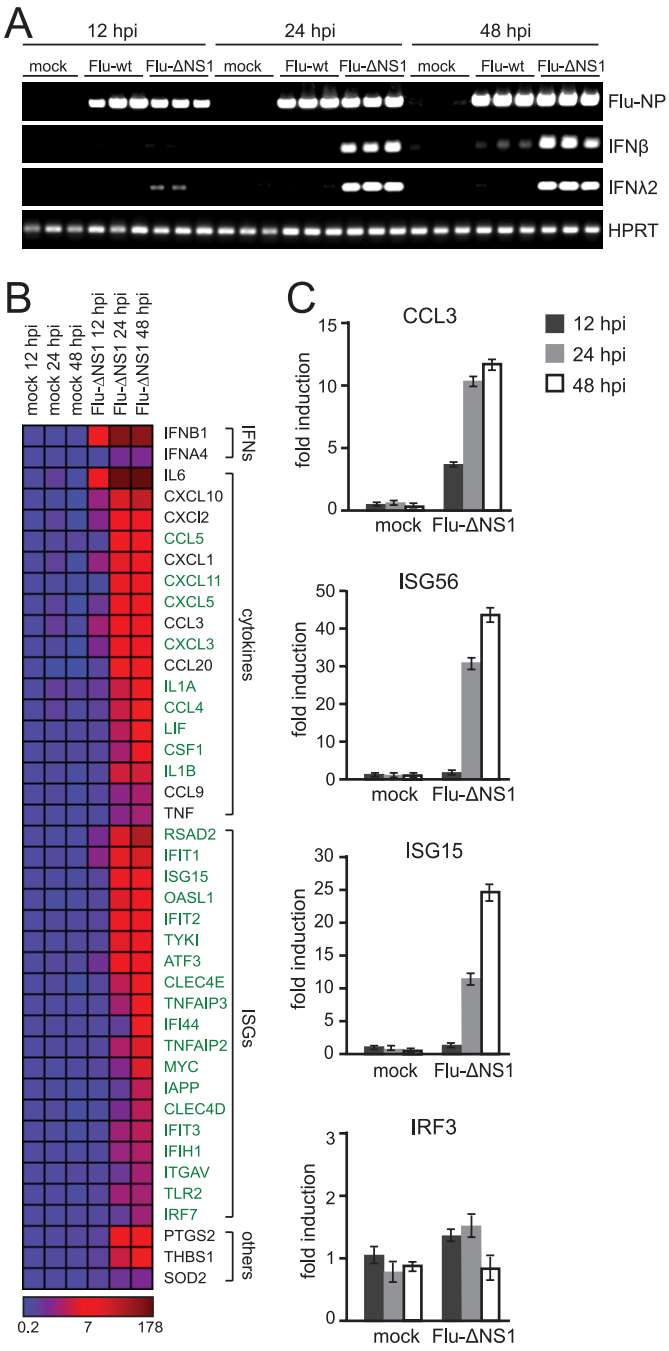

FIGURE 1. **Virus induced genes in mice deficient in IFNAR1 and IL28Rα.** *A*, IFNAR1$^{-/-}$IL28Rα$^{-/-}$ double knock-out mice were mock treated or infected intranasally with 10^5 pfu of SC35M-wt (Flu-wt) or SC35M-ΔNS1 (Flu-ΔNS1). 12, 24, and 48 hpi, three mice per treatment were sacrificed and total lung RNA was isolated. RT-PCR with primers specific for the viral nucleoprotein (Flu-NP), IFNβ, IFNλ2, and hypoxanthine guanine phosphoribosyl transferase (*HPRT*) was performed. *B*, RNA of three lungs per treatment was pooled and standard affymetrix analysis was performed. The heat map depicts fold induction of genes compared with lungs from mock-treated animals at 12 hpi. ISGs are shown in *green*. *C*, transcript quantities of chemokine (C-C motif) ligand 3 (CCL3), interferon-stimulated gene 56 (ISG56/interferon-induced protein with tetratricopeptide repeats IFIT2), ISG15, and IRF3, determined by qPCR. Fold induction is relative to mock-treated samples at 12 hpi ± S.D.

infected, mice. Of note, other ISGs such as Mx1 were not upregulated under these conditions. Subsequent validation of the array was confirmed by qPCR (Fig. 1*C*).

Given the activation of IRF3/7 in response to an NS1-deficient influenza A virus infection (50), transcriptional induction, in the absence of IFN signaling, presumably reflects the activity of these transcription factors. This is supported by the observation that IFNβ is highly induced in response to Flu-ΔNS1, a gene requiring the cooperative binding of two heterodimeric IRF3/IRF7 complexes (21). It however is surprising that, in addition to IFNβ, many virus-inducible genes have also been characterized as ISGs (marked in *green* in Fig. 1*B*) despite the complete loss of ISGF3 activity. These results suggest that the paradigm of antiviral signaling being the transcriptional consequence of IFN-mediated ISGF3 activation is incorrect and that a layer of redundancy exists to induce a similar transcriptome, presumably to aid in the intracellular combat against viral infection.

Defining Sequence Requirements for IRF-specific, ISGF3-specific, or Universal ISREs—As the predicted protein:DNA contacts occupied by IRF3/7 and ISGF3 share many common bases within their respective DNA binding motifs, we speculated that IRF7 may perform functionally redundant roles to ISGF3. IRF7, unlike IRF3, is more promiscuous in its DNA binding (30), is inducible by IFN (36), and is found at high basal concentrations only in critical viral response cells such as pDCs (35, 52). To address this question, we aimed to identify an ISRE that could be bound by both ISGF3 and IRF7 with relative equal affinities. For these purposes, we focused on the manipulation of a well-characterized ISRE motif from the IFN-stimulated gene 15 (ISG15) (40, 41, 53). To this end, IRF7 or the components of ISGF3 (STAT1, STAT2, IRF9) were exogenously produced in fibroblasts and activated with either IKKϵ or IFNβ (Fig. 2*A*). To check functionality of the exogenous proteins, we performed a reporter assay utilizing an ISG15 ISRE-dependent luciferase construct. Expression of IRF7 or ISGF3, in the absence of stimulation, did not result in significant activation; however, activation of IRF7 with IKKϵ or ISGF3 with either IKKϵ or IFNβ led to strong induction of luciferase (Fig. 2*B*). This activity correlated to the engagement of an ISG15 ISRE oligonucleotide as measured by electromobility shift assay (EMSA) (Fig. 2*C*). IRF7 bound to the ISG15 ISRE as a homodimer, but not as a heterodimer with IRF3, as only an antibody generated against the Flag-tagged IRF7, but not against IRF3, could modulate the migration of the complex (Fig. 2*C*). ISGF3 migration was impacted by antibodies against STAT1, STAT2, and IRF9, confirming formation of a functional ISGF3 complex (Fig. 2*C*). Furthermore, IRF9 binding to the oligonucleotide could be easily detected by EMSA, presumably as a monomer based on molecular mass, even in the absence of IFN treatment (Fig. 2*C*). Monomeric IRF9 binding is inversely correlated to the assembly of ISGF3 in which the additional binding of STAT1 and STAT2 is greatest in the presence of IFNβ and IKKϵ as previously described (13). Taken together, these data demonstrate that the exogenous expression and activation of IRF7 and ISGF3 reconstitutes a valid model to study binding redundancies between these transcription factors.

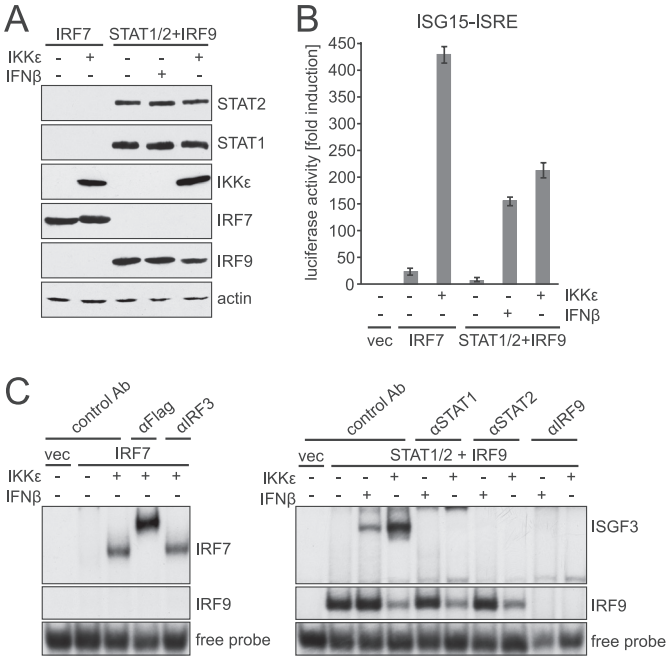

FIGURE 2. **Correlating transcriptional activity to IRF7/ISGF3 ISRE binding.** Extracts from fibroblasts exogenously expressing IRF7 or the components of ISGF3 (STAT1, STAT2, IRF9) were analyzed by Western blot (*A*), by expression of luciferase from an ISG15-ISRE-dependent reporter construct (*B*), and by binding to an ISG15-ISRE oligonucleotide by EMSA (*C*). Expression of IKKϵ or treatment with IFNβ was used to activate IRF7 or ISGF3. Empty vector (*vec*) served as control. *B*, average fold induction of luciferase activity over vec $\pm$ S.D. Protein composition of the complexes bound to the ISRE in *C* was analyzed using antibodies specific to Flag, IRF3, STAT1, STAT2, IRF9, or control antibody (*Ab*).

To ascertain the requirements for IRF7 and ISGF3 binding, we performed EMSAs on the aforementioned IRF7 and ISGF3 extracts beginning first with the wild-type ISG15 ISRE (ISG15wt, Fig. 3*A*). This ISRE element corresponds with the enhancer used in the luciferase reporter shown in Fig. 2*B*. The ISG15-ISRE consists of two overlapping ISRE core sequences as defined by the GAAA motif found in characterized ISRE and IRF-E sites (Fig. 3*A*, *blue box*). Surprisingly, while the ISG15 ISRE encodes a complete ISGF3 (GAAANNGAAACT (5) and IRF motif (AANNGAAANNGAAA (14)) the probe itself was found to only strongly associate with IRF7. To further refine the binding sites of IRF7 and ISGF3, and to ascertain whether overlap between the transcription factor motifs is evident, we began by minimizing the ISG15 ISRE to a single core sequence flanked with adjacent nucleotides (nts) from the human ISG15-promoter (*gray boxes* in Fig. 3*B*, ISG15core^{+wt} in which the core is referenced as nt 1–12, the 5′-flanking sequence -1 to -7, and the 3′-flanking region $+1$ to $+8$). Motif minimization resulted in minimal reduction of IRF7 binding but a significant increase in the binding of ISGF3 and IRF9 (Fig. 3*B*). Interestingly, randomizing the flanking sequences of the minimal motif (*red boxes* in Fig. 3*C*, ISG15core$^{+5\prime\text{-}3\prime\text{random}}$) did not affect IRF7 binding but abolished ISGF3 and IRF9 binding further supporting the notion that there are IRF7-specific sequences and confirming that an ISGF3 ISRE has sequence requirements that extend beyond the consensus motif (Fig. 3*C*). Changing the 3′-flanking sequence back to wt (Fig. 3*D*, ISG15core$^{+5\prime\text{random}}$) did rescue

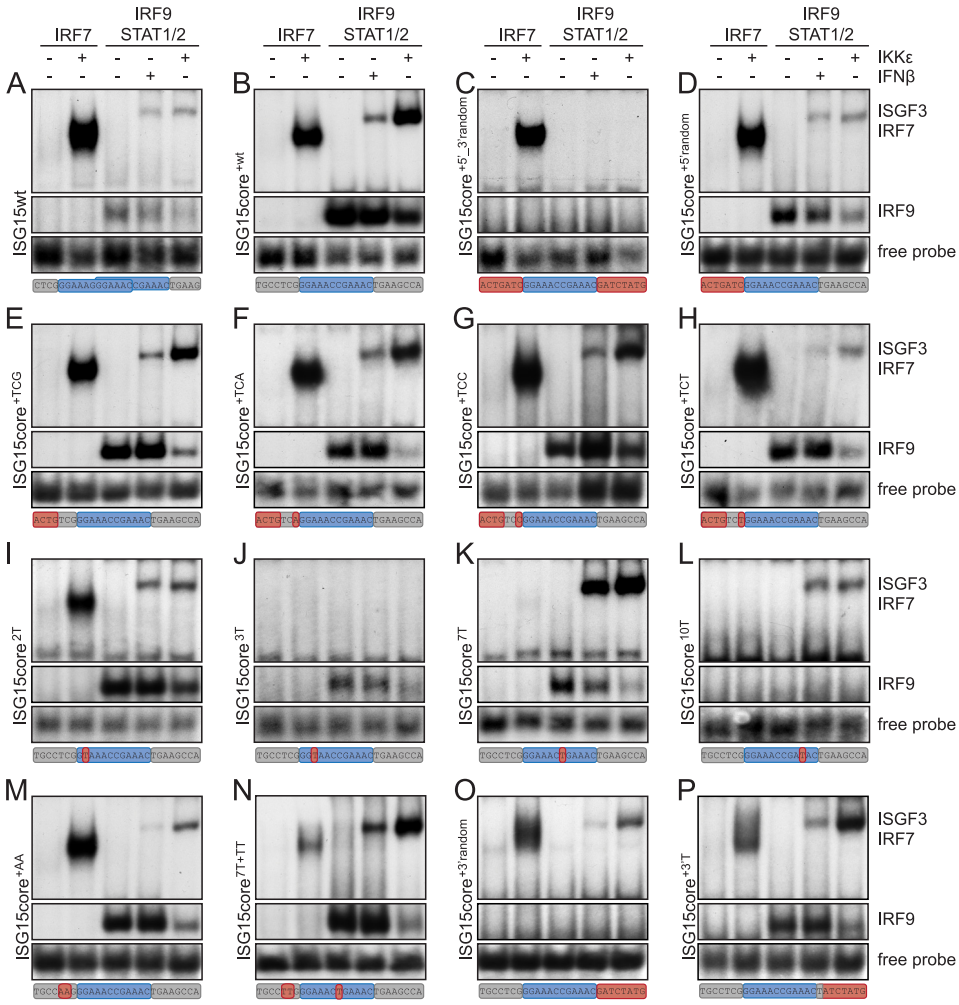

FIGURE 3. **Systematic analysis of DNA binding of IRF7 and ISGF3.** *A–P*, EMSAs were performed with extracts derived from fibroblasts exogenously expressing IRF7 and IKKε or the components of ISGF3 in the presence of IFNβ or IKKε. Respective probes for depicted EMSAs can be found *beneath* each panel. *Blue* depicts the ISRE core sequence, *gray*, the flanking wild-type sequences, and *red*, introduced nucleotide changes.

limited binding of ISGF3 and IRF9 as compared with ISG15core$^{+5'\text{-}3'\text{random}}$, but it failed to reach the binding capacity observed for ISG15core^{+wt}. Not surprising, IRF7 binding was not affected by the 3′-flanking sequence (Fig. 3*D*).

To delineate the sequence requirements for ISGF3 further, we maintained the endogenous 3′-flanking sequence and partially restored the 5′-adjacent nts ATC to TCG (ISG15core$^{+5'TCG}$, Fig. 3*E*) to determine what effect this would have on the binding of ISGF3. While binding of IRF7 or IRF9 was not affected when comparing ISG15core^{+wt} to ISG15core$^{+5'TCG}$, the affinity of ISGF3 to this motif was still lower than to ISG15core^{+wt} but increased as compared with ISG15core$^{+5'random}$. In contrast, changing the remaining 4 nt of the 5′-flanking sequence did not impact ISGF3 binding (supplemental Fig. S1). Further analysis of the −1 to −3 position demonstrated that while a variety of bases were amenable for ISGF3 binding, a T at the −1 position, an A at the −2 position, or a C or G at the −3 position significantly limited ISGF3 binding strongly suggesting that ISGF3 binds the major groove at this location (Fig. 3, *E–H* and supplemental Fig. S2).

We next analyzed the nucleotide contribution of the ISRE core as it relates to the binding of IRF7 and ISGF3. To execute these studies, we systematically replaced each of the core nts with T's and ascertained the impact these substitutions had on IRF7 and ISGF3 binding (Fig. 3, *I–L* and supplemental Fig. S3). Fig. 3, *I–L* shows four examples of nucleotides that define IRF7 and/or ISGF3 specificity. Some mutations, like ISG15core^{2T} (Fig. 3*I*) did not affect IRF7 or IRF9 binding, but reduced binding of ISGF3; thus, showing nucleotides that make contact to STAT1. Furthermore, some mutations such as position 3, abolish binding of IRF7 and ISGF3 but have only a moderate affect on IRF9 binding (Fig. 3*J*). Mutation of position 7 completely abolishes IRF7 binding, reduces IRF9 binding, but does not affect ISGF3 (Fig. 3*K*). Last, mutation of position 10 abolishes IRF7 and IRF9 binding, but maintains a weak association with ISGF3 (Fig. 3*L*).

Taken together, this mutational analysis suggests an IRF7-binding consensus is encoded by the sequence AAWNC-GAAA (W = A/T), which differs slightly from the published sequence AANNGAAANNGAAA. To ascertain the importance of the first two bases at the −2 and −3 position, we replaced both bases in ISG15core^{+wt} with As and found no impact on IRF7 binding, in contrast to ISGF3 (Fig. 3*M*). Taken together with the results of Fig. 2, *A–H*, it would appear that

IRF7 binds the minor groove at this position, making contact only at the −3 position. We next investigated whether nucleotides at position −2 and −3 influenced IRF7 binding in the context of an unfavorable ISRE-core. We therefore changed the C at position 7, previously found to be critical for IRF7 binding (Fig. 3*K*), and combined this with the predefined optimal AA or TT nt at positions −2 and −3 (Fig. 3*N*). Interestingly, this probe analysis demonstrated that optimal binding in the minor groove at positions −2 and −3 can compensate for suboptimal binding in the major groove at position 7.

Finally, we determined which nucleotides in the 3′-flanking region are important for ISGF3 binding. Mutation of the 3′-flanking sequence reduced binding of ISGF3 compared with the wild-type ISG15 probe (Fig. 3*O*). This loss of binding was likely the result of a loss of IRF9 binding as the randomized 3′-flanking sequence also inhibited IRF9 engagement (Fig. 3*O*). This is supported by the fact that reversion of position +1 to a T, rescued IRF9 binding and increased ISGF3 affinity for the ISRE (Fig. 3*P*). Binding analysis for IRF3 on all of these probes demonstrated only moderate stimulus-specific binding on ISG15wt, ISG15core^{+AA}, and ISG15core^{7T+TT} in agreement with past studies regarding IRF3 binding requirements (26, 30).

In summary, this body of work demonstrates that an ISRE can demonstrate both, transcription factor specificity or redundancy. Furthermore, IRF7 and ISGF3, both multimeric protein complexes, show plasticity in the DNA contacts they require for stable occupancy. Taken together, these data suggest that the minimal DNA-binding motif of IRF7 is AAWNCGAAA, but WWNNGAAANNGAAA can also confer IRF7 binding compatibility. The detailed consensus of ISGF3 is WBVGGAANNGAAACT (B = C/G/T, V = A/C/G). While only changes at the underlined nucleotide completely abolish ISGF3 binding on this consensus, single changes at other sites were found to reduce overall binding.

Defining the IRF7 transcriptome in the Absence of IFN-I and -III Signaling—In an effort to determine whether the ISRE redundancy observed *in vivo* in IFNAR1$^{-/-}$IL28R$\alpha^{-/-}$ double knock-out mice and *in vitro* by EMSA could be correlated to *in vivo* IRF7 activity, we performed an additional microarray in human cells, which were also deficient in IFN signaling. To this end, we utilized the 2FTGH-derived human fibrosarcoma cell line U3A, which is deficient in STAT1 and, consequently IFN-I and IFN-III signaling (Fig. 4, *A* and *B* (46). To determine whether activation of IRF7 demonstrated the same extensive overlap with ISGF3 observed *in vitro*, we exogenously expressed IRF7 or IRF7 and IKKϵ. As expected, IKKϵ-mediated activation of IRF7 in U3A cells resulted in robust ISRE binding and expression of IFNα1 without subsequent synthesis of IFN-dependent MxA, which is an ISG known to be dependent on IFN and not directly responsive to IRFs (54) (Fig. 4*B*).

To ascertain the IRF7 transcriptome in the absence of IFN signaling, exogenous expression of GFP was compared with expression of IRF7 and IKKϵ by standard affymetrix gene array (Fig. 4*C*). IFNβ was also added to both conditions to eliminate any non-canonical signaling induced by IFNβ-mediated, STAT1-independent signaling. Not surprisingly, gene array

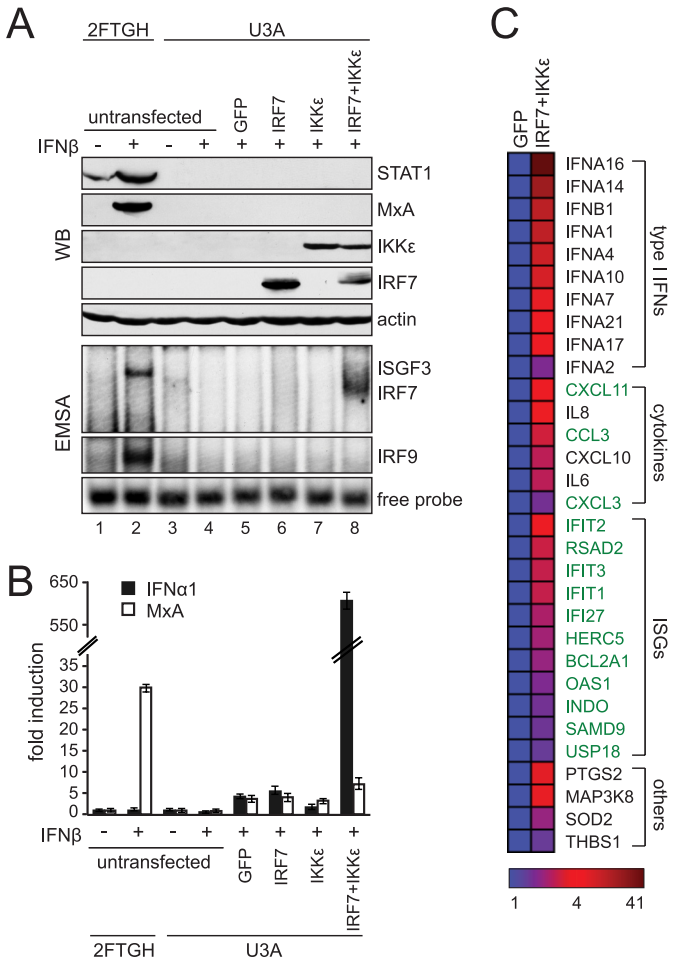

FIGURE 4. **Affymetrix analysis of STAT1-independent IRF7-induced genes.** *A*, Western blot and binding analysis of 2FTGH and U3A extracts from mock or IFNβ-treated cells exogenously expressing the indicated combinations of GFP, IRF7, and IKKϵ. EMSA was performed with an ISG15-ISRE probe. *B*, qPCR from samples described in *A* for IFNα1 and myxovirus (influenza) resistance A (*MxA*). The graph depicts average fold induction over untreated cells ± S.D. *C*, affymetric analysis of total RNA of U3A cells treated with IFNβ in addition to exogenous expression of either GFP or IRF7 and IKKϵ. ISGs are shown in *green*.

analysis of IRF7- and IKKϵ-expressing cells demonstrated the induction of previously characterized IRF3-regulated genes, namely the members of the IFN-inducible p56 family (IFN-induced protein with tetratricopeptide repeats 1 IFIT1/ISG56, IFIT2/ISG54, and IFIT3/ISG60) (39–41), and radical *S*-adenosyl methionine domain containing 2 (RSAD2) (41). However, in addition to this subset, IRF7 activation resulted in cytokine induction (including IFN-I, as previously described (25, 26, 31, 52), as well as a large subset of genes previously thought to be dependent on IFN-I signaling (Fig. 4*C*, ISGs marked in *green*). These genes include IFIT5, IFN-induced with helicase C domain 1 (IFIH1), guanylate-binding protein IFN-inducible 1 (GBP1), 2′-5′-oligoadenylate synthetase 2 (OAS2), OAS-like (OASL), and IRF9 in addition to those listed (Fig. 4*C*). In fact, taken together, ~80% of the genes up-regulated by IRF3/7 in U3A cells were also up-regulated in mice upon infection with Flu-ΔNS1 (as shown in Fig. 1*B*) suggesting that the functional redundancy between IRF3/7 and ISGF3 is evolutionary conserved among vertebrates.

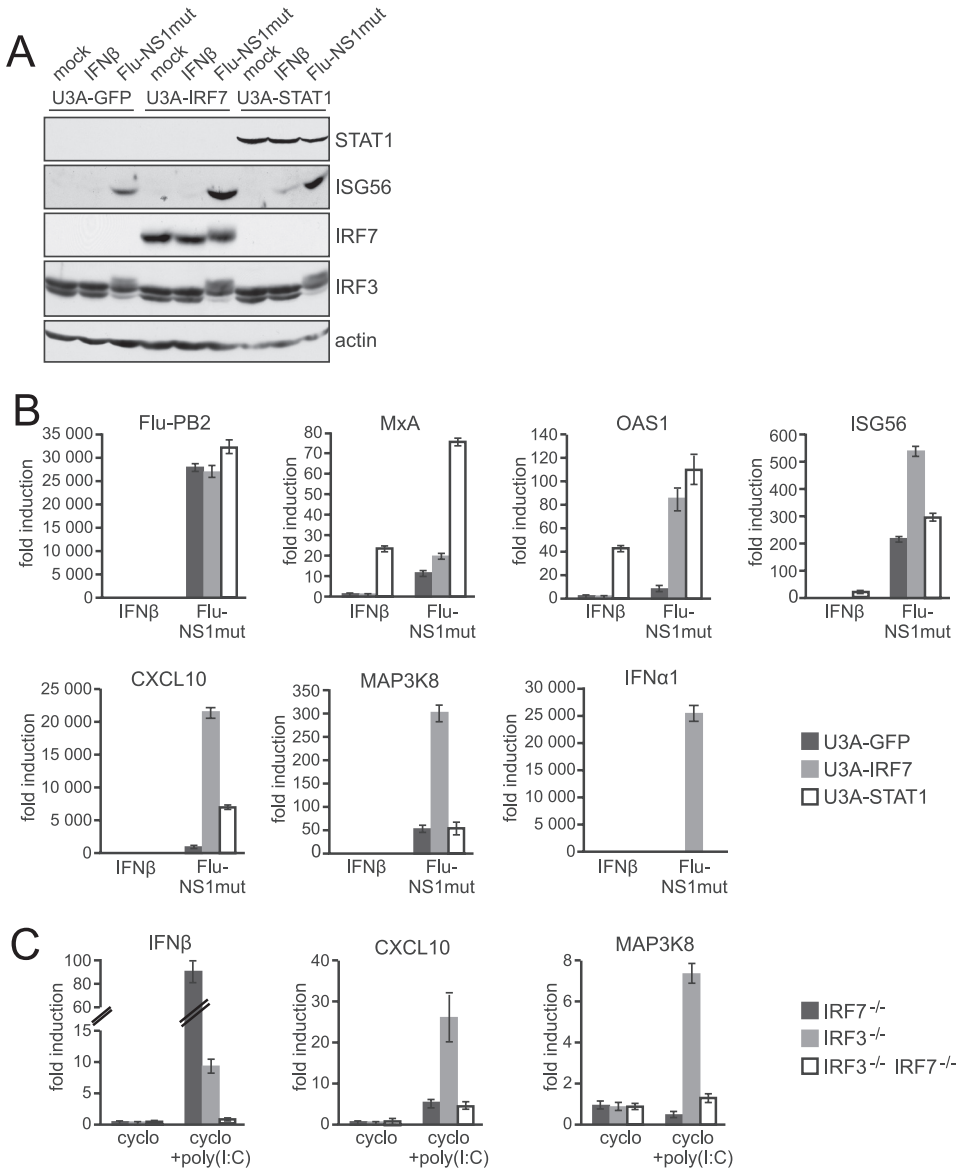

FIGURE 5. **ISRE-specific expression of virus-inducible genes.** *A*, U3A cells stably expressing GFP, IRF7, or STAT1 were treated with IFNβ or infected at an MOI of 5 with an influenza A virus mutant harboring two amino acid changes in the NS1 protein (Flu-NS1mut). Western blot analysis was performed 8 h post-treatment. *B*, qPCR analysis of cells treated with Flu-NS1mut or IFNβ (10 h post-treatment). Depicted qPCR products include: PB2 (Flu-PB2), MxA, 2′,5′-oligoadenylate synthetase 1 (OAS1), ISG56, chemokine (CXC motif) ligand 10 (CXCL10), mitogen-activated protein kinase kinase kinase kinase 8 (MAP3K8), and IFNα1. The graph depicts average fold induction over mock-treated U3A-GFP cells $\pm$ S.D. *C*, primary MEFs from Irf7$^{-/-}$, Irf3$^{-/-}$, and Irf3$^{-/-}$Irf7$^{-/-}$ mice were treated with poly(I:C) to activate endogenous IRF3 or IRF7, respectively. In addition, the cells were treated with cycloheximide (*cyclo*) to inhibit translation and thereby prevent IFN signaling. qPCR was performed 8 h post-treatment. The graph depicts average fold induction over primary MEFs treated with cyclo only $\pm$ S.D.

IRF7-specific, ISGF3-specific, and Universal ISREs in the Promoters of ISGs—To confirm the IRF7 and ISGF3 transcriptomes, U3A cells stably expressing GFP (U3A-GFP), IRF7 (U3A-IRF7), or STAT1 (U3A-STAT1) were treated with IFNβ or infected with an influenza A strain, harboring a mutation in NS1 that renders NS1 incapable of preventing activation of IRF3/IRF7 (Flu-NS1mut) (45) (Fig. 5*A*). Western blot analysis demonstrated IRF3-dependent induction of ISG56 in U3A-GFP cells upon virus infection, a response that was further enhanced in U3A-IRF7 cells. Furthermore, reconstitution of STAT1 in U3A cells restored IFN-responsiveness of ISG56, also demonstrating an enhancement following virus infection as compared with U3A-GFP control cells. To corroborate the redundancy of the IFN- and IRF-mediated transcriptomes in this model system, total RNA from IFNβ or virus treated samples was isolated and analyzed by qPCR. As we found virus replication levels to be comparable at 10 hpi, we profiled IRF7-dependent genes and compared these to MxA, a hallmark for ISGs (Fig. 5*B*). These data demonstrated that MxA was induced in U3A-STAT1 cells upon IFNβ-treatment alone and further up-regulated in infected U3A-STAT1 cells, presumably due to a synergistic cooperation between ISGF3 and another virus activated factor (Fig. 5*B*). In contrast, OAS1, which is strongly induced in U3A-STAT1 cells upon IFNβ treatment, was also induced in virus-infected U3A-IRF7 cells. In addition, knock-down of endogenous IRF3 in U3A-

TABLE 1
ISRE sequences of IRF7-regulated genes

Gene	ISRE sequence	Position[a]	Ref.
IRF7-regulated			
CXCL10	TTTG GAAA GT GAAA CC	−224/−208	(57)
IL6	AAAA GAAA AAA GAAA GT	−269/−253	(58)
CXCL3	*ACGC TAAA CC GAAA AT*	−455/−439	
IFIT2/ISG54	AAGG GAAA GT GAAA CT	−84/−100	(19)
RSAD2	AATA GAAA CA GAAA TG	−952/−968	
IFIT1/ISG56	TAGG GAAA CC GAAA GGG GAAA GT GAAA CT	−90/−118	(59)
IFI27	*CCAG GAAA CC GAAA CT*	−95/−111	(60)
HERC5	*AGTG GAAA AC GAAA CA*	−58/−74	
BCL2A1	AAAA GAAA A GAAA AT	−914/−930	
OAS1	*TGAG GAAA C GAAA CC*	−103/−88	(19)
SAMD9	AAAT GAAA CT GAAA CC	−94/−110	
USP18	AATG GAAA GC GAAA CT	+83/+67	
ISGF3 only			
MxA	CGAA GAAA T GAAA CT	−40/−57	(56)

[a] Position of the ISRE sequence in correlation to the transcriptional start site.

IRF7 cells did not significantly reduce induction of OAS1 (supplemental Fig. S4). These results suggest that OAS1 is predominantly regulated by ISGF3 and IRF7, but not by the ubiquitous IRF3. Furthermore, induction of ISG56 in U3A-STAT1 cells in response to IFNβ is low, compared with its induction by viral infection, suggesting that IRF3 and IRF7 are stronger inducers of ISG56 than ISGF3. Last, CXCL10, MAP3K8, and IFNα1 are not expressed upon IFNβ-treatment, but all demonstrate robust induction in U3A-IRF7 cells. In addition, knock-down of endogenous IRF3 suggested, that IRF7 can efficiently drive transcription of CXCL10, MAP3K8, and IFNα1 in the absence of IRF3 (supplemental Fig. S4). To further address IRF7-dependent gene expression in a different model system, we used primary MEFs from Irf7$^{-/-}$, Irf3$^{-/-}$, and Irf3$^{-/-}$Irf7$^{-/-}$ mice. As previously described (52), activation of endogenous IRF3 or IRF7 in Irf7$^{-/-}$ or Irf3$^{-/-}$ primary MEFs, respectively, leads to induction of IFNβ, whereas Irf3$^{-/-}$Irf7$^{-/-}$ primary MEFs are incapable of IFNβ production (Fig. 5*C*). Furthermore, only Irf3$^{-/-}$, but not Irf7$^{-/-}$ or Irf3$^{-/-}$Irf7$^{-/-}$ primary MEFs express high levels of CXCL10 and MAP3K8 upon poly(I:C) stimulation (Fig. 5*C*). This gene induction is not due to autocrine/paracrine IFN-I signaling, as primary MEFs were additional treated with cycloheximide to inhibit translation. Taken together, these results demonstrate that the IRFs are capable of inducing a broad array of genes that demonstrate significant overlap with ISGs as well as including a unique subset of gene products.

To ascertain whether the optimal DNA binding sequence for IRF7 accurately accounted for the IRF7-induced transcriptome, we analyzed the genomic sequence upstream of the IRF7-dependent transcriptional start sites. In support of the biochemical studies, we were able to divide the identified genes into two distinct categories: one subset that contained the sequence WWNNGAAANNGAAA (Table 1) and another which lacked A/T base pairing in the minor groove of position −2 and −3 (marked in italics in Table 1). The promoters of this latter group conformed to the sequence AAWNCGAAA. In contrast, the ISRE of MxA does not conform to the required minor groove consensus at the −2 and −3 positions, nor does it encode a C inbetween the two GAAA repeats.

To test binding of IRF3, IRF7, and ISGF3 to the ISREs of IRF7-regulated genes, we exogenously expressed each of the

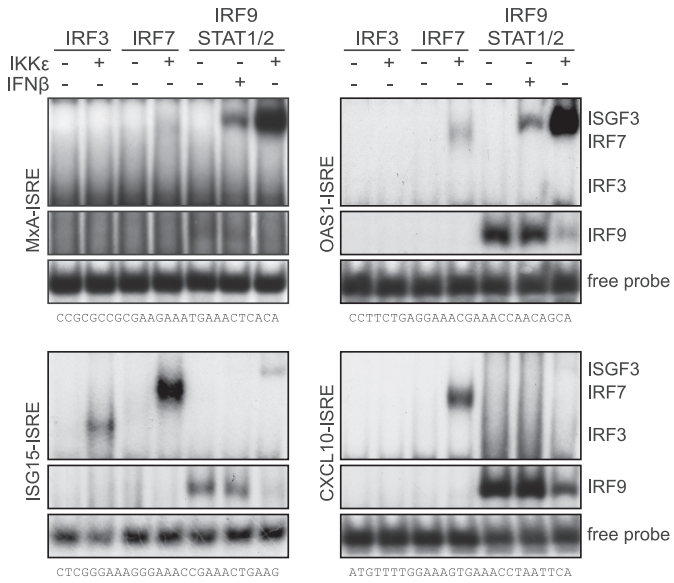

FIGURE 6. **IRF3-, IRF7-, and ISGF3-specific binding of human ISREs.** EMSAs were performed with extracts from fibroblasts exogenously expressing IRF3, IRF7, or ISGF3 in addition to IKKϵ or IFNβ. EMSA probe sequences are depicted *below* each corresponding panel.

three transcription factor complexes independently and analyzed the putative ISREs by EMSA. As expected, the MxA-ISRE bound ISGF3 but not IRF3 or IRF7 (Fig. 6 and supplemental Fig. S5). In contrast, IRF7 and ISGF3, but not IRF3, bound to the OAS1-ISRE. The ISG15-ISRE is a more promiscuous ISRE, binding IRF3, IRF7, and ISGF3, whereas only IRF7 demonstrated strong binding to the CXCL10-ISRE. Although IRF3/7 heterodimer formation cannot be ruled out, analysis of IRF3 knock-down and Irf3$^{-/-}$ primary MEFs, suggest that IRF7 homodimers dominate in transcribing a significant portion of the "ISG transcriptome". To ensure that this binding activity, produced by the ectopic expression of IRF7, was reflective of endogenous activity, we analyzed IFN-treated cells, stimulated with poly(I:C) to ascertain binding patterns of the IRFs *versus* that of ISGF3 (supplemental Fig. S6*A*). For this analysis we incubated extracts with the CXCL10-ISRE and identified a single inducible factor, which could only be supershifted by an IRF7 antibody (supplemental Fig. S6*B*). Taken together, this endogenous IRF7-specific

binding, validates the model derived from ectopic expression and the data conferred from virus-infected lung tissue.

DISCUSSION

The type I IFN system is an essential component for inhibiting virus replication. It relies on the recognition of the pathogen leading to downstream signaling events and secretion of IFNβ. IFNβ in turn induces the assembly and activation of ISGF3 in an autocrine and paracrine manner, which up-regulates a set of antiviral ISGs, thereby conferring an antiviral state to a cell. In addition to this, so-called viral stress-inducible genes (VSIG) are directly induced by PAMPs in the infected cell and do not depend on IFNβ signaling. The transcription factors suggested to be responsible for induction of VSIGs are nuclear factor of κ light polypeptide gene enhancer in B-cells (NFκB), activator protein 1 (AP1) and IRF3/IRF7 (53). Here we delineate the transcriptional profiles of ISGs and VSIGs through *in vitro* biochemistry and *in vivo* validation.

The enhancer elements responsible for the transcriptional induction of ISGs and VSIGs are often referred to simply as ISREs. However, no distinction is presently made between an ISRE that binds to IRFs, ISGF3, or both factors. Here we have defined the *in vitro* biochemical and *in vivo* transcriptional requirements of a universal ISRE *versus* an ISGF3- or IF7-specific ISRE. We found that the DNA binding properties of ISGF3 and IRF7 both demonstrate some levels of plasticity. For the IRF7 dimer, a perfect consensus sequence for one subunit (AAWNCGAAA) is sufficient for both binding and transcriptional induction, but mismatches in this region can be compensated for by AT base pairing in the neighboring upstream minor groove. In a similar manner non-canonical ISREs mismatched at almost any position by a single base, demonstrate ISGF3-binding, presumably due to additional DNA:STAT1/2 contacts upstream of the core motif. In contrast, the IRF3 dimer demonstrates a more restricted DNA binding specificity, as it demands conservation for both of its ISRE half-sites (28, 30). This difference is probably due to an extended loop in the DNA binding domain of IRF7 but not IRF3, providing more flexibility to engage in additional protein-protein interactions and direct contacts with the DNA (15). In agreement with the sequence requirements, we show that the transcriptional response to virus infection is defined by the ISREs encoded upstream of target genes. These include motifs that permit binding of IRF3, IRF7, and ISGF3, IRF7 and ISGF3, demonstrate transcription factor specificity, or simply encode multiple ISREs in a single promoter (10, 38, 54–56). Taken together the detailed definition of sequence requirements for transcriptional activity of IRF3, IRF7, and ISGF3 should allow computational prediction based on the levels of these three factors.

As IRF3 and ISGF3 are found ubiquitously, it follows that the level of IRF7 is an important factor in determining a cellular transcriptional response to virus infection. In fact, IRF7 has already been termed the "master regulator" for its essential role in the induction of IFN-I (52). This body of work supports this finding but extends IRF7 function beyond the simple induction of a single gene product. As IRF7 is undetectable in most non-hematopoietic cells, initial induction of IFNβ is likely the result of two sets of IRF3 dimers assembled within the context of the enhanceosome (15). As the ISREs of the IFNβ enhancer (termed positive regulatory domains (PRD) I and III) are imperfect, dependence on IRF3 alone results in stochastic gene expression in a very small subset of cells (36, 37). Low levels of IFNβ, as well as additional virus-induced cytokines, prime neighboring cells to induce IRF7 and subsequent viral spread results in greater induction of IFNβ mediated by IRF3/IRF7 heterodimers (21). It is also the elevated basal expression of IRF7 that permits pDCs to secrete high levels of IFNβ *in vivo* (52). Here we demonstrate that, in addition to IFNβ secretion, pDCs and primed non-lymphoid cells would also be inherently more resistant to virus infection. The presence of IRF7, whether basal or the result of priming, would confer an ISGF3-like transcriptome onto the cells, thereby establishing a less permissive environment for viral replication with shorter kinetics. With this in mind, it is perplexing why IRF7 expression does not mimic that of IRF3 as this would no doubt confer greater overall cellular resistance to viral infection. Perhaps the expression of IRF7 is confined to a subset of cells to prevent unnecessary IFN-I secretion and induction of the antiviral state by demanding a certain level of viral replication before being induced. Given our constant environmental exposure to viruses that pose no threat, constitutive IRF7 would result in an unnecessary transcriptional response ultimately resulting in systematic toxicity.

Acknowledgments—The following reagent was obtained through the National Institutes of Health Biodefense and Emerging Infections Research Resources Repository, NIAID, National Institutes of Health: Human Interferon Beta (HuIFN-β), NR-3080.

REFERENCES

1. Pestka, S., Krause, C. D., and Walter, M. R. (2004) *Immunol. Rev.* **202,** 8–32
2. García-Sastre, A., and Biron, C. A. (2006) *Science* **312,** 879–882
3. Haller, O., Kochs, G., and Weber, F. (2007) *Cytokine Growth Factor Rev.* **18,** 425–433
4. O'Shea, J. J., Gadina, M., and Schreiber, R. D. (2002) *Cell* **109, (**suppl.), S121–131
5. Darnell, J. E., Jr., Kerr, I. M., and Stark, G. R. (1994) *Science* **264,** 1415–1421
6. Zhou, Z., Hamming, O. J., Ank, N., Paludan, S. R., Nielsen, A. L., and Hartmann, R. (2007) *J. Virol.* **81,** 7749–7758
7. Dumoutier, L., Tounsi, A., Michiels, T., Sommereyns, C., Kotenko, S. V., and Renauld, J. C. (2004) *J. Biol. Chem.* **279,** 32269–32274
8. Reich, N., Evans, B., Levy, D., Fahey, D., Knight, E., Jr., and Darnell, J. E., Jr. (1987) *Proc. Natl. Acad. Sci. U.S.A.* **84,** 6394–6398
9. Shirayoshi, Y., Burke, P. A., Appella, E., and Ozato, K. (1988) *Proc. Natl. Acad. Sci. U.S.A.* **85,** 5884–5888
10. Rutherford, M. N., Hannigan, G. E., and Williams, B. R. (1988) *EMBO J.* **7,** 751–759
11. Kessler, D. S., Levy, D. E., and Darnell, J. E., Jr. (1988) *Proc. Natl. Acad. Sci. U.S.A.* **85,** 8521–8525
12. Cohen, B., Peretz, D., Vaiman, D., Benech, P., and Chebath, J. (1988) *EMBO J.* **7,** 1411–1419
13. tenOever, B. R., Ng, S. L., Chua, M. A., McWhirter, S. M., García-Sastre, A., and Maniatis, T. (2007) *Science* **315,** 1274–1278
14. Fujii, Y., Shimizu, T., Kusumoto, M., Kyogoku, Y., Taniguchi, T., and

Hakoshima, T. (1999) *EMBO J.* **18,** 5028–5041
15. Escalante, C. R., Nistal-Villán, E., Shen, L., García-Sastre, A., and Aggarwal, A. K. (2007) *Mol. Cell* **26,** 703–716
16. Seeman, N. C., Rosenberg, J. M., and Rich, A. (1976) *Proc. Natl. Acad. Sci. U.S.A.* **73,** 804–808
17. Brierley, M. M., and Fish, E. N. (2005) *J. Biol. Chem.* **280,** 13029–13036
18. Chen, X., Vinkemeier, U., Zhao, Y., Jeruzalmi, D., Darnell, J. E., Jr., and Kuriyan, J. (1998) *Cell* **93,** 827–839
19. Tanaka, N., Kawakami, T., and Taniguchi, T. (1993) *Mol. Cell. Biol.* **13,** 4531–4538
20. Paun, A., and Pitha, P. M. (2007) *Biochimie* **89,** 744–753
21. Panne, D., Maniatis, T., and Harrison, S. C. (2007) *Cell* **129,** 1111–1123
22. Panne, D., Maniatis, T., and Harrison, S. C. (2004) *EMBO J.* **23,** 4384–4393
23. Veals, S. A., Santa Maria, T., and Levy, D. E. (1993) *Mol. Cell. Biol.* **13,** 196–206
24. Escalante, C. R., Yie, J., Thanos, D., and Aggarwal, A. K. (1998) *Nature* **391,** 103–106
25. Sato, M., Hata, N., Asagiri, M., Nakaya, T., Taniguchi, T., and Tanaka, N. (1998) *FEBS Lett.* **441,** 106–110
26. Marié, I., Durbin, J. E., and Levy, D. E. (1998) *EMBO J.* **17,** 6660–6669
27. Taniguchi, T., Ogasawara, K., Takaoka, A., and Tanaka, N. (2001) *Annu. Rev. Immunol.* **19,** 623–655
28. Morin, P., Bragança, J., Bandu, M. T., Lin, R., Hiscott, J., Doly, J., and Civas, A. (2002) *J. Mol. Biol.* **316,** 1009–1022
29. Driggers, P. H., Ennist, D. L., Gleason, S. L., Mak, W. H., Marks, M. S., Levi, B. Z., Flanagan, J. R., Appella, E., and Ozato, K. (1990) *Proc. Natl. Acad. Sci. U.S.A.* **87,** 3743–3747
30. Lin, R., Génin, P., Mamane, Y., and Hiscott, J. (2000) *Mol. Cell. Biol.* **20,** 6342–6353
31. Sato, M., Suemori, H., Hata, N., Asagiri, M., Ogasawara, K., Nakao, K., Nakaya, T., Katsuki, M., Noguchi, S., Tanaka, N., and Taniguchi, T. (2000) *Immunity* **13,** 539–548
32. Baum, A., and García-Sastre, A. (2010) *Amino Acids* **38,** 1283–1299
33. Sharma, S., tenOever, B. R., Grandvaux, N., Zhou, G. P., Lin, R., and Hiscott, J. (2003) *Science* **300,** 1148–1151
34. Au, W. C., Moore, P. A., Lowther, W., Juang, Y. T., and Pitha, P. M. (1995) *Proc. Natl. Acad. Sci. U.S.A.* **92,** 11657–11661
35. Izaguirre, A., Barnes, B. J., Amrute, S., Yeow, W. S., Megjugorac, N., Dai, J., Feng, D., Chung, E., Pitha, P. M., and Fitzgerald-Bocarsly, P. (2003) *J. Leukoc. Biol.* **74,** 1125–1138
36. Lu, R., Au, W. C., Yeow, W. S., Hageman, N., and Pitha, P. M. (2000) *J. Biol. Chem.* **275,** 31805–31812
37. Lu, R., Moore, P. A., and Pitha, P. M. (2002) *J. Biol. Chem.* **277,** 16592–16598
38. Wang, N., Dong, Q., Li, J., Jangra, R. K., Fan, M., Brasier, A. R., Lemon, S. M., Pfeffer, L. M., and Li, K. (2010) *J. Biol. Chem.* **285,** 6080–6090
39. Peters, K. L., Smith, H. L., Stark, G. R., and Sen, G. C. (2002) *Proc. Natl. Acad. Sci. U.S.A.* **99,** 6322–6327
40. Grandvaux, N., Servant, M. J., tenOever, B., Sen, G. C., Balachandran, S., Barber, G. N., Lin, R., and Hiscott, J. (2002) *J. Virol.* **76,** 5532–5539
41. Andersen, J., VanScoy, S., Cheng, T. F., Gomez, D., and Reich, N. C. (2008) *Genes Immun.* **9,** 168–175
42. Barnes, B. J., Richards, J., Mancl, M., Hanash, S., Beretta, L., and Pitha, P. M. (2004) *J. Biol. Chem.* **279,** 45194–45207
43. Mordstein, M., Kochs, G., Dumoutier, L., Renauld, J. C., Paludan, S. R., Klucher, K., and Staeheli, P. (2008) *PLoS Pathog.* **4,** e1000151
44. Kochs, G., Koerner, I., Thiel, L., Kothlow, S., Kaspers, B., Ruggli, N., Summerfield, A., Pavlovic, J., Stech, J., and Staeheli, P. (2007) *J. Gen. Virol.* **88,** 1403–1409
45. Donelan, N. R., Basler, C. F., and García-Sastre, A. (2003) *J. Virol.* **77,** 13257–13266
46. McKendry, R., John, J., Flavell, D., Müller, M., Kerr, I. M., and Stark, G. R. (1991) *Proc. Natl. Acad. Sci. U.S.A.* **88,** 11455–11459
47. Niwa, H., Yamamura, K., and Miyazaki, J. (1991) *Gene* **108,** 193–199
48. Evans, M. J., von Hahn, T., Tscherne, D. M., Syder, A. J., Panis, M., Wölk, B., Hatziioannou, T., McKeating, J. A., Bieniasz, P. D., and Rice, C. M. (2007) *Nature* **446,** 801–805
49. Perez, J. T., Varble, A., Sachidanandam, R., Zlatev, I., Manoharan, M., García-Sastre, A., and tenOever, B. R. (2010) *Proc. Natl. Acad. Sci. U.S.A.* **107,** 11525–11530
50. Hale, B. G., Randall, R. E., Ortin, J., and Jackson, D. (2008) *J. Gen. Virol.* **89,** 2359–2376
51. Wolff, T., and Ludwig, S. (2009) *J. Interferon Cytokine Res.* **29,** 549–557
52. Honda, K., Yanai, H., Negishi, H., Asagiri, M., Sato, M., Mizutani, T., Shimada, N., Ohba, Y., Takaoka, A., Yoshida, N., and Taniguchi, T. (2005) *Nature* **434,** 772–777
53. Sarkar, S. N., and Sen, G. C. (2004) *Pharmacol. Ther.* **103,** 245–259
54. Holzinger, D., Jorns, C., Stertz, S., Boisson-Dupuis, S., Thimme, R., Weidmann, M., Casanova, J. L., Haller, O., and Kochs, G. (2007) *J. Virol.* **81,** 7776–7785
55. Severa, M., Coccia, E. M., and Fitzgerald, K. A. (2006) *J. Biol. Chem.* **281,** 26188–26195
56. Asano, A., Jin, H. K., and Watanabe, T. (2003) *Gene* **306,** 105–113
57. Luster, A. D., and Ravetch, J. V. (1987) *Mol. Cell. Biol.* **7,** 3723–3731
58. Sancéau, J., Kaisho, T., Hirano, T., and Wietzerbin, J. (1995) *J. Biol. Chem.* **270,** 27920–27931
59. Wathelet, M. G., Lin, C. H., Parekh, B. S., Ronco, L. V., Howley, P. M., and Maniatis, T. (1998) *Mol. Cell* **1,** 507–518
60. Martensen, P. M., Søgaard, T. M., Gjermandsen, I. M., Buttenschon, H. N., Rossing, A. B., Bonnevie-Nielsen, V., Rosada, C., Simonsen, J. L., and Justesen, J. (2001) *Eur. J. Biochem.* **268,** 5947–5954